Surface roughness development during photoresist dissolution

Lewis W. Flanagin,[a] Vivek K. Singh,[b] and C. Grant Willson[c]
Department of Chemical Engineering, The University of Texas at Austin, Austin, Texas 78712
and Technology CAD Department, Intel Corporation, Hillsboro, Oregon 97124-6497

(Received 16 February 1999; accepted 14 May 1999)

The minimization of nanoscale roughness in patterned images has become a priority for the process of photolithography in the production of microprocessors. In order to probe the molecular basis for surface roughness, the development of photoresist has been simulated through application of the critical-ionization model to a three-dimensional molecular lattice representation of the polymer matrix. The model was adapted to describe chemically amplified photoresists of the sort now commonly used in microlithography. Simulations of the dependence of the dissolution rate and surface roughness on the degree of polymerization, polydispersity, and fractional deprotection agree with experimental results. Changes in surface roughness are shown to correlate with the length of the experimentally observed induction period. Model predictions for the effect of void fraction and developer concentration on roughness are also presented. Observations of differences in the effect of developer concentration on top-surface and sidewall roughness are explained by a critical development time predicted by the simulation. © *1999 American Vacuum Society.*
[S0734-211X(99)06704-9]

I. INTRODUCTION

The tremendous gain in computational speed and storage capacity afforded by miniaturization of the integrated circuit impels the semiconductor industry forward in its quest for smaller device features. The demands placed on microlithography grow more arduous with each new generation of microprocessors. The minimization of roughness associated with the surface and edges of photoresist images now stands as one of the challenges to continued advances in lithographic technology.

The problems of top-surface and line-edge roughness have drawn a considerable amount of attention within the last year, and several recent atomic force microscopy (AFM) studies have yielded notable insights into the process dependency of photoresist roughness. He and Cerrina[1] have studied the relationship between surface roughness and exposure dose over a range of postexposure bake times for a positive-tone chemically amplified photoresist. Their results indicate that systems having the same overall average degree of deprotection, but different process histories, exhibit similar surface morphologies, but different degrees of roughness. Reynolds and Taylor[2–4] have explored the responses of top-surface and sidewall roughness for chemically amplified photoresists to a variety of processing parameters, including exposure dose and developer concentration. They find that higher exposure doses and lower developer concentrations lead to decreased surface roughness, but their measurements of sidewall roughness show no correlation with their surface roughness results and reveal a negligible dependence of sidewall roughness on either exposure dose or developer concentration. Yoshimura *et al.*[5] have characterized the effects of the polymer structure and molecular weight distribution on edge roughness. They show that a photoresist based on cresol novolac exhibits a rougher surface than one based on polyvinylphenol and attribute this difference in roughness to the greater structural rigidity of cresol novolac that results from the presence of aromatic rings in the backbone of the polymer. They observe that polymers having lower molecular weight and lower polydispersity produce less roughness.

The need for robust lithographic simulators that can model and predict the generation of roughness during photoresist development grows imperative. Most of the earlier simulations of photoresist development do not adequately describe surface roughness because they considered the photoresist a uniform structure. Guerrieri and Neureuther[6] have studied the time evolution of the development etch front using a simplified material crack model in which development proceeds faster along highly exposed filaments (cracks) than through the background matrix, and they have found that the surface roughness increases with crack length. Trefonas[7] alludes to the production of top-surface roughness during his molecular cell-based simulations of percolational development. Scheckler *et al.*[8] have used an even more advanced molecular-scale photoresist development simulation in which a realistic polymer chain length distribution is represented to demonstrate excellent agreement between their model and AFM measurements for the dose dependence of surface roughness. These studies have made significant advancements in the simulation of roughness in photoresist development, yet they still rely heavily on empirical data for the dependence of the dissolution rate on such fundamental quantities as molecular weight and degree of deprotection.

Our simulations represent the polymer matrix as a three-dimensional rectangular lattice in which each lattice cell corresponds exactly to a polymer repeat unit. The lattice cells are strung together to form polymer chains via random walks as described previously.[9] The dissolution of these chains is governed by the critical-ionization model,[10] which proposes

---

[a] Present address: The University of Texas at Austin.
[b] Present address: Intel Corporation.
[c] Corresponding author; electronic mail: willson@che.utexas.edu

that a critical fraction of segments on a chain must be in the ionized state in order for the chain to dissolve. The lattice model has been adapted to represent a chemically amplified photoresist system in which each cell begins as either a chemically protected (blocked) group or a chemically deprotected (unblocked) group. In a previous paper, we presented simulations of photoresist dissolution on a two-dimensional (2D) grid.[9] Because percolation models have demonstrated a dependence on the dimensionality of the system,[6,7] we have extended the moving front from a line to a surface, which begins parallel to the substrate. Adding the third dimension alters the quantitative results, but not the qualitative behavior, of our system. The third dimension (3D) allows a greater number of possible chain conformations and a greater number of cell faces that may be exposed to developer (six instead of four).

The simulations described in this article allow polymer blends so that we can study the effects of polydispersity. An initial void fraction, which can represent either the inherent polymer free volume or residual casting solvent, is also specified. The molecular-level model correctly predicts trends in the responses of the dissolution rate and roughness to changes in the degree of polymerization, polydispersity, degree of deprotection, polymer free volume, residual casting solvent, and development time.

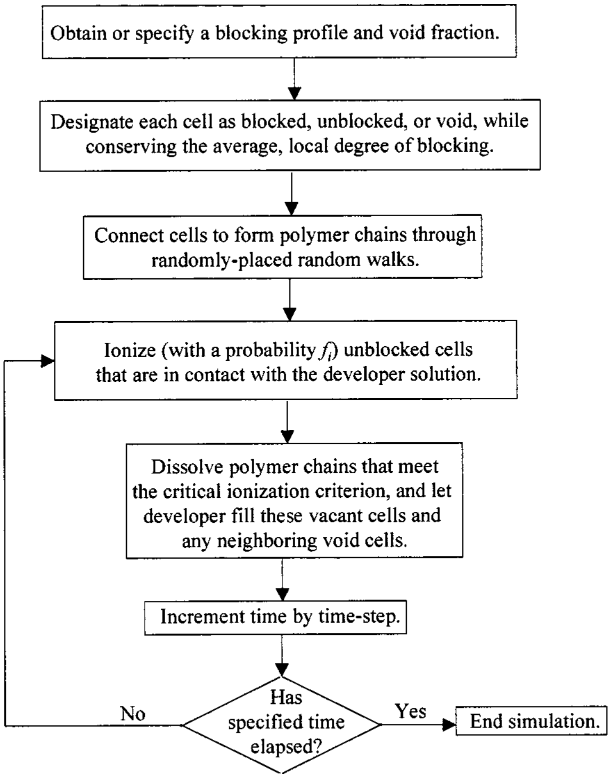

FIG. 1. Flowchart for the three-dimensional molecular simulation.

II. MODEL DESCRIPTION

A three-dimensional lattice of cubic cells is used to represent the polymer matrix. The number of cells in each orthogonal direction is 73. Each lattice cell, having sides of 0.7 nm in length, corresponds exactly to a single repeating unit of a polymer chain and may have one of the following states: blocked, unblocked, ionized, developed, or void. The initial degree of blocking, specified by the user, is designated f_{b0}. For a blanket (uniform) exposure, the value of f_{b0} represents the average degree of blocking present in the entire lattice. For a patterned photoresist image, f_{b0} represents the average degree of blocking prior to exposure; the spatial variation in blocking, $f_b(x,y,z)$, prior to dissolution is the product of f_{b0} and $p(x,y,z)$, a function with values between 0 and 1. The function $p(x,y,z)$ describes the relative amount of protection remaining after exposure and the postexposure bake and is supplied by FINLE Technology's PROLITH, one of several commercially available lithographic simulators. The initial void fraction, also specified by the user, is designated f_v. The void fraction can represent either the polymer's inherent free volume or residual casting solvent. A flowchart describing the steps in the molecular model simulation is shown in Fig. 1.

Prior to development, a fraction f_v of the cells are selected at random to be void. Each of the remaining cells is designated randomly as either blocked or unblocked, where the probability of being blocked is given by $f_b/(1-f_v)$. This expression for the probability of being blocked ensures that the average local concentration of blocked sites is preserved through the random selection process. The accuracy of the discrete representation of the continuous function $f_b(x,y,z)$ is checked by examining the average amount of blocking over an area and comparing this against the scalar-field value supplied. (The number of cells used in the average is chosen so that their combined volume is the same as the cellular volume in the PROLITH blocking profile.) As in our 2D simulations,[9] statistical variation is introduced through the transformation of the continuous polymer matrix into a molecular grid. However, such roughness is expected from the statistical variation in the energy that is deposited into the photoresist during exposure.[11]

The simulation requires having polymer chains on the grid. The user specifies values (DP_i) for the degree of polymerization and the fraction of chains (f_{DPi}) that are supposed to have each degree of polymerization. To form these chains, the cells are strung together[12] via random walks, which are begun in randomly chosen blocked or unblocked cells that have not already been used in the formation of other chains. The number of steps taken in each walk equals one of the nominal degrees of polymerization specified by the user in the input file. The fraction of walks with DP_i steps is given by f_{DPi}. The random walks avoid the cells designated as void (or filled with solvent), but more than one chain may share any given blocked or unblocked cell (Fig. 2). A cell may be counted as belonging to any single chain only once; thus, there are no repeated cells within any given chain. This precaution leads to a distribution of actual chain lengths. The formation of chains continues until all blocked or unblocked cells have become a part of at least one chain. If only one degree of polymerization is specified, the random walk process produces a Gaussian distribution of actual chain lengths

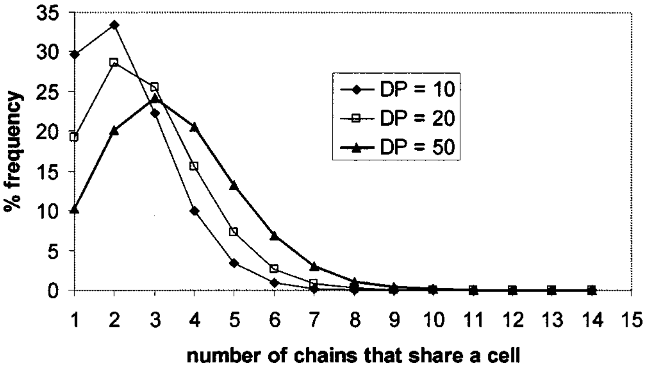

FIG. 2. Distribution in the number of chains that share a cell as a function of the specified degree of polymerization.

[Fig. 3(a)]. The chain length distribution for 2D is shown also for comparison. The additional third dimension narrows the chain length distribution and shifts it towards greater chain lengths (which will presently be explained). If two degrees of polymerization are specified, a bimodal distribution results [Fig. 3(b)], where the distribution about each mode is Gaussian.

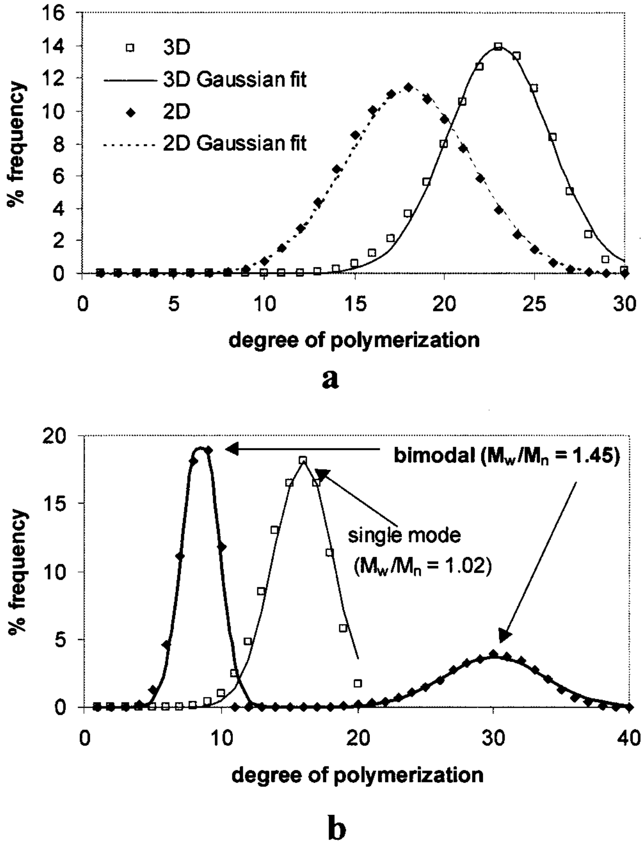

FIG. 3. (a) Polymer chain length distributions produced through the random walk process when a nominal (maximum) chain length of 30 is specified for 3D and 2D simulations. (b) Two polymer chain length distributions having the same average degree of polymerization (15.5) but different polydispersity (DP=20 for the single-mode distribution; $\mathrm{DP}_1=10$, $\mathrm{DP}_2=40$, and $f_{\mathrm{DP1}}=0.6589$ for the bimodal distribution).

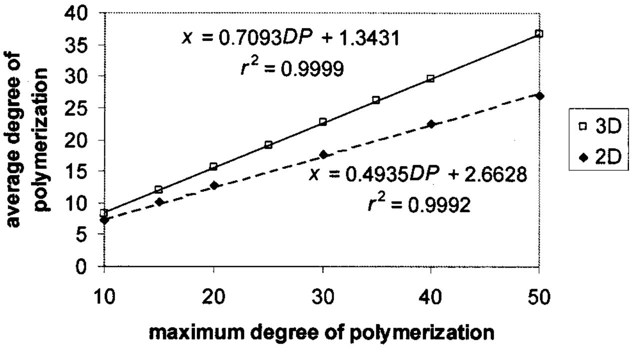

FIG. 4. Relationship between the maximum degree of polymerization (DP) and the average degree of polymerization (x) from the random walk process. Note that the r^2 values are the squares of the linear correlation coefficients for the least-squares linear regression of the data.

The average (or mean) degree of polymerization is easily obtained from the chain length distribution. In Fig. 4, the average degree of polymerization is plotted versus the maximum degree of polymerization, which is identically equal to the specified number of steps to be taken in the formation of each chain. The corresponding plot for two dimensions is also shown. The range of chain lengths that is shown here, 10–50 repeat units, is representative of the oligomeric, phenolic polymers used to formulate photoresists. Note that the process produces a linear relationship between the average and maximum degrees of polymerization. The third dimension increases the average degree of polymerization because the extra degree of freedom in the third dimension reduces the average number of redundant steps taken during the random walks and increases the probability for a growing chain to encounter an available cell. The random walk process produces a polymer size distribution that is uniform throughout most of the film, but that has slightly smaller values towards the ends (Fig. 5).

The mean-squared radius of gyration, $\langle R_g^2\rangle$, and mean-squared end-to-end distance, $\langle R^2\rangle$, are common measures for the polymer chain length. Calculated values for $\langle R_g^2\rangle$ and $\langle R^2\rangle$ from our simulations, shown in Fig. 6, exhibit the linear dependence on the degree of polymerization expected for dense polymer networks.[13] The ratio $\langle R^2\rangle/\langle R_g^2\rangle$ (Table I) is close to the theoretical value of 6.[13]

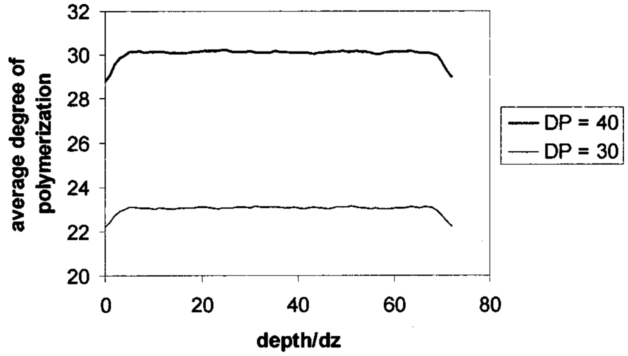

FIG. 5. Variation in the average degree of polymerization with depth into the film.

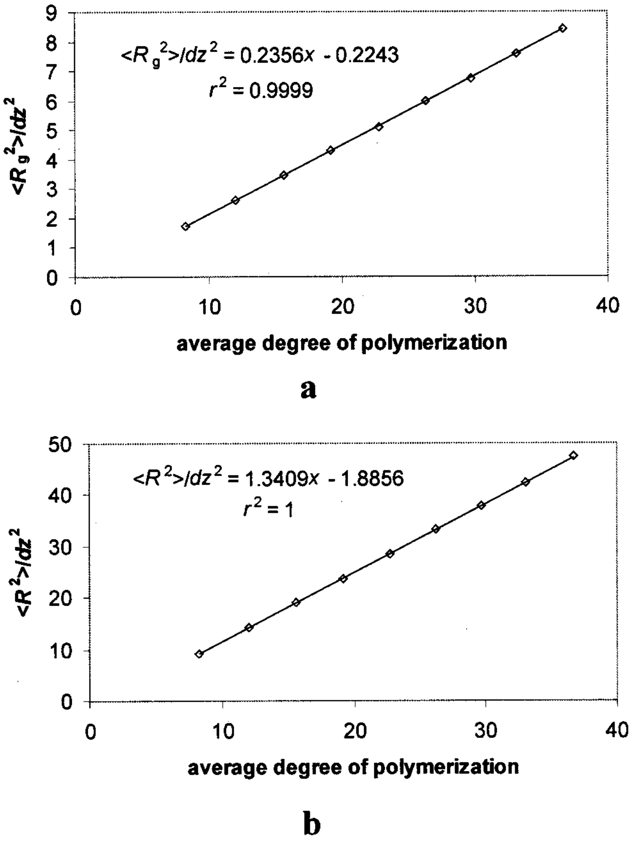

FIG. 6. Measures of polymer chain length as a function of the average degree of polymerization (x): (a) mean-squared radius of gyration, $\langle R_g^2\rangle$, and (b) mean-squared end-to-end distance, $\langle R^2\rangle$. Note that the r^2 values are the squares of the linear correlation coefficients for the least-squares linear regression of the data.

Once polymer chains have completely filled the grid, the simulator begins the process of ionization. All cells on the top layer of the lattice are always exposed to developer. Ionization is possible for all top-layer cells that are in the unblocked state, and any top-layer cells that are in the void state automatically fill with developer. Unblocked cells that are adjacent to developed cells may also undergo ionization. Whether ionization actually occurs depends on the probability of ionization (f_i), a factor specified by the user that depends on the concentration of the developer and the pK_a of the resin.[14,15]

TABLE I. Ratio of mean-squared end-to-end distance to mean-squared radius of gyration as a function of maximum degree of polymerization.

DP	$\langle R^2\rangle/\langle R_g^2\rangle$
10	5.36
15	5.46
20	5.50
25	5.53
30	5.60
35	5.58
40	5.61
45	5.58
50	5.64

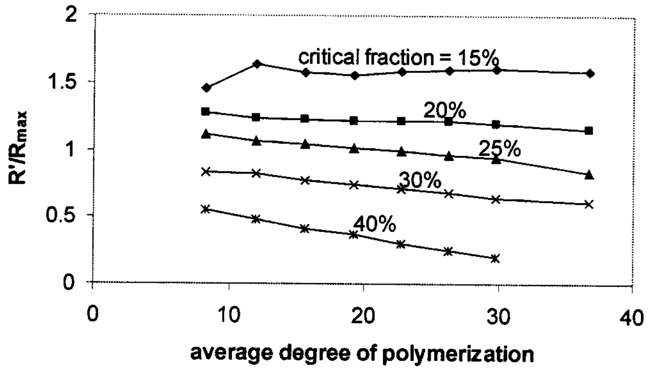

FIG. 7. Correction factor by which the time step must be multiplied in order to obtain the specified $R_{\max}$ when $f_{b0}=0$, $f_v=0$, and $f_i=0.5$.

After the ionization step, each chain is examined to see if it has the requisite fraction of ionized sites for dissolution (f_c). At the end of this accounting, all chains meeting the solubility criterion are dissolved (erased). If a cell is shared by at least one other chain, it remains in its current state (blocked or unblocked); otherwise, the cell is counted as developed. The cycle of ionization followed by dissolution continues until the time specified by the user has elapsed. The time (t_c) that each cycle represents is given by

$$t_c=\frac{dz}{R_{\max}}(R'/R_{\max}). \tag{1}$$

Here dz is the cell height, $R_{\max}$ is the experimental dissolution rate observed under complete exposure, and $R'/R_{\max}$ is a correction factor added to ensure that the rate calculated by the simulator when $f_{b0}=0$ is $R_{\max}$. (For an ideal monomer system with $f_{b0}=0$ and $f_i=1$, $R'/R_{\max}=1$ because one entire layer dissolves during each ionization/dissolution cycle. $R'/R_{\max}$ is a measure of the deviation from this ideality.) Figure 7 shows how $R'/R_{\max}$ varies with the critical degree of ionization and average degree of polymerization. A detailed description of $R'/R_{\max}$ is given elsewhere.[9]

The spatial average and the standard deviation of the thickness of remaining photoresist are computed during the simulation. The surface roughness is defined throughout this article as the standard deviation in the spatial variation of the photoresist thickness. Results for surface roughness, r, and remaining thickness, θ, versus time, t, are presented as averages from multiple simulations using different seeds for the random number generator that fills the lattice. The purpose of running multiple simulations is to sample a larger subspace of the total ensemble of possible spatial configurations, and standard deviations of the results are provided to show reproducibility. Dimensionless variables are used wherever possible. Lengths are scaled by the cell height (dz), and time is scaled by the time per ionization/dissolution cycle [Eq. (1)].

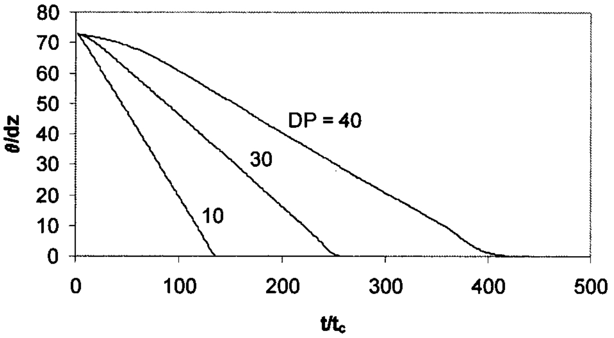

FIG. 8. Effect of the nominal degree of polymerization, DP, on a dimensionless plot of the average thickness of polymer film remaining, θ, vs time, t ($f_c=0.4$, $f_{b0}=0$, $f_v=0$, $f_i=0.5$). Each curve is the result of averaging seven simulations.

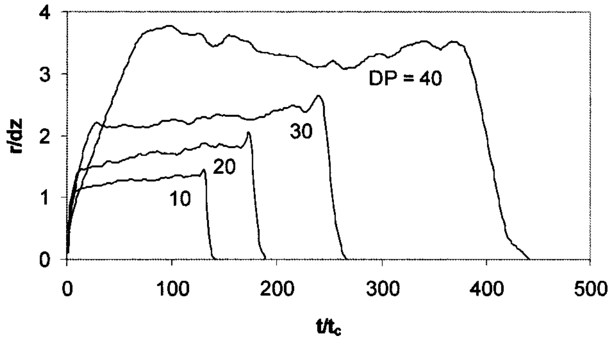

FIG. 9. Effect of the nominal degree of polymerization, DP, on a dimensionless plot of roughness, r, vs time, t ($f_c=0.4$, $f_{b0}=0$, $f_v=0$, $f_i=0.5$). Each curve is the result of averaging seven simulations.

III. SIMULATION RESULTS

A. Effect of the degree of polymerization

In Fig. 8, the remaining thickness of a fully deprotected polymer is plotted versus development time for several nominal degrees of polymerization. The model predicts that the dissolution rate decreases with increasing degree of polymerization. Many experimental studies confirm this result.[16–20] The instantaneous dissolution rate is given by the negative of the slope from a plot of thickness versus time ($-d\theta/dt$, where θ = thickness and t = time). The instantaneous rate is constant over most of the course of dissolution, but interesting deviations in $d\theta/dt$ occur at the start and end of the process. The time that the system takes to achieve a constant dissolution rate is called the induction period. This phenomenon, which is observed experimentally, appears ‘‘naturally’’ in the simulation. Because the instantaneous rate is smaller at both the top and bottom surfaces of the film, surface rate inhibition is said to occur at both interfaces. Dissolution rates are customarily defined as the instantaneous rate when half of the initial film thickness remains. This arbitrary definition minimizes the effect of surface inhibition, and is adopted for the purposes of this article.

From Fig. 8, it is apparent that surface rate inhibition becomes more pronounced as the degree of polymerization increases. All of these systems display an induction period, but the length of the induction period increases faster than a linear dependence on the degree of polymerization would predict. The surface rate inhibition at the bottom film surface also grows with the degree of polymerization, but the dependence is not as steep at the bottom as it is at the top.

The variation in average thickness across simulations (not shown) increases until developer reaches the region where bottom-surface rate inhibition occurs, and the most rapid increase occurs during the top-surface induction period. The results indicate that the variation among runs rises significantly with an increase in the degree of polymerization.

Surface roughness as a function of development time and degree of polymerization is plotted in Fig. 9 for the system described in Fig. 8. In agreement with the experimental results of Yoshimura *et al.*,[5] the simulation results show that surface roughness increases with increasing degrees of polymerization. For all degrees of polymerization, the same general behavior is observed: roughness rises sharply at first, reaches a plateau with a general slight incline, spikes, and then rapidly falls. This trend is compatible with AFM measurements that we have taken for the time evolution of surface roughness (Table II). Variation in surface roughness across multiple simulations (not shown) increases with degree of polymerization, and a spike occurs at the same location as the spike in surface roughness. A comparison between Figs. 8 and 9 reveals that the initial, sharp rise in roughness corresponds exactly to the induction period of the dissolution rate and that the final spike in roughness occurs where bottom-surface rate inhibition begins.

The correspondence between surface rate inhibition and surface roughness in our simulations helps to explain the surface rate inhibition phenomenon. An increase in roughness, by definition, occurs when the surface area exposed to developer increases. When dissolution begins, the film surface is flat, and the area exposed to developer is the smallest it will be during the entire process. As chains dissolve away, a greater surface area is exposed, which leads to increases in the surface roughness and the instantaneous dissolution rate. The amount of surface area that may be exposed at any time reaches a nearly constant value, after which point the instantaneous dissolution rate and surface roughness stay relatively constant. When developer finally reaches the bottom of the film, the surface area in contact with developer decreases rapidly, and both the surface roughness and dissolution rate

TABLE II. Surface roughness as a function of development time[a] (rms=root mean square).

Development time (s)	Thickness remaining (nm)	rms roughness (nm)
0	1089	0.3
25	999	3.8
50	807	3.8

[a] Polymer: *m*-cresol novolac, cast with PGMEA at 3000 rpm for 30 s, baked at 120 °C for 120 s, developed with 0.182N TMAH for the time indicated, rinsed with distilled water, and blown dry with nitrogen. The surface roughness was calculated from AFM images taken on a Park Scientific Instruments Autoprobe.

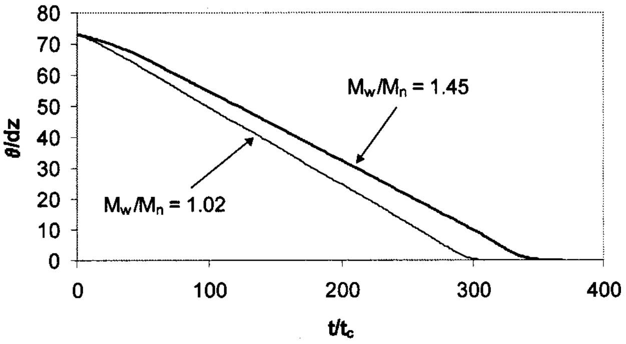

FIG. 10. Effect of polydispersity, M_w/M_n, on a dimensionless plot of the average thickness of polymer film remaining, θ, vs time, t ($f_c=0.4$, $f_{b0}=0.1$, $f_v=0$, $f_i=0.5$). The polymer chain length distribution for each curve is shown in Fig. 3. Each curve is the result of averaging seven simulations.

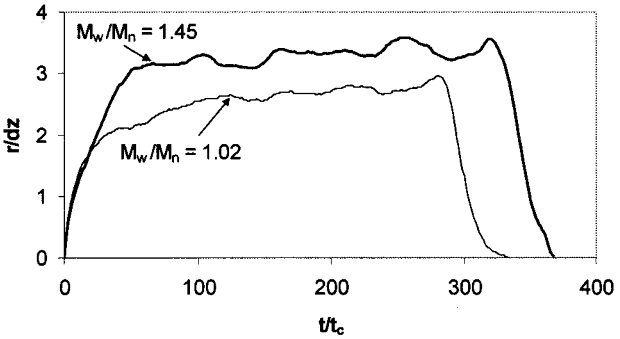

FIG. 11. Effect of polydispersity, M_w/M_n, on a dimensionless plot of roughness, r, vs time, t ($f_c=0.4$, $f_{b0}=0.1$, $f_v=0$, $f_i=0.5$). The polymer chain length distribution for each curve is shown in Fig. 3. Each curve is the result of averaging seven simulations.

decline. Thus, both the induction period and bottom-surface rate inhibition arise from rapid changes in surface roughness. Similar arguments have been used to explain surface rate inhibition in percolation models.[7]

B. Effect of polydispersity

In Fig. 3(b), a single-mode and a bimodal polymer chain length distribution, which have the same average degree of polymerization but different polydispersity, are compared. The single-mode distribution has a narrower chain length distribution and a lower polydispersity ($M_w/M_n=1.02$) than the bimodal distribution ($M_w/M_n=1.45$).

Experimental efforts to determine the effect of polydispersity on the dissolution rate have led to conflicting results. Tsiartas *et al.*[1] measured the dissolution rates of blends of fractionated novolacs and found that the dissolution rate of the novolac blends decreased with increasing polydispersity. A similar study by Barclay *et al.*[2] concluded that increasing the polydispersity of (higher molecular weight) poly(hydroxystyrene) leads to higher dissolution rates. Figure 10 depicts the predictions from our simulations for the dissolution rate of the chain distributions shown in Fig. 3(b). According to our model, the lower-polydispersity polymer dissolves faster than the polymer blend, which has a wider molecular-weight distribution. In agreement with the conclusions of Tsiartas *et al.*, the simulations suggest that higher molecular-weight fractions have a disproportionately large influence on the overall dissolution rate.

Figure 11 shows how surface roughness develops in these two systems. In agreement with the experimental results of Yoshimura *et al.*,[5] the higher-polydispersity sample achieves a greater degree of surface roughness. The time that the system requires for the degree of surface roughness to level increases with polydispersity and corresponds to the induction period in Fig. 10. Thus, increasing the polydispersity enhances the effect of surface rate inhibition. Those who formulate resists have recognized this phenomenon for some time, but there has been no satisfying explanation for the observation.

C. Effect of the degree of deprotection

The time evolution of surface roughness as a function of the degree of blocking, f_{b0}, is depicted in Fig. 12. The simulations predict that roughness should increase with the degree of blocking as long as the film is able to clear. The dissolution rate decreases with increasing degrees of blocking. After a critical degree of blocking is exceeded (e.g., $f_{b0}=0.23$ for DP=10), the film cannot completely clear, and a measure of roughness remains even after the film stops developing. For a completely protected system (i.e., $f_{b0}=1$), none of the film clears, and no surface roughness develops. Thus, surface roughness begins at zero, passes through a maximum, and returns to zero as the fractional deprotection is varied from 0 to 1. This point is illustrated by Fig. 13, where the predictions of our model for roughness as a function of deprotection at a set development time are compared to the experimental data of He and Cerrina.[1] The relationship between exposure dose and fractional deprotection has been quantified previously.[21] Figure 14 demonstrates that very little clearing occurs at low doses (or at high degrees of blocking) in both simulation and experiment.

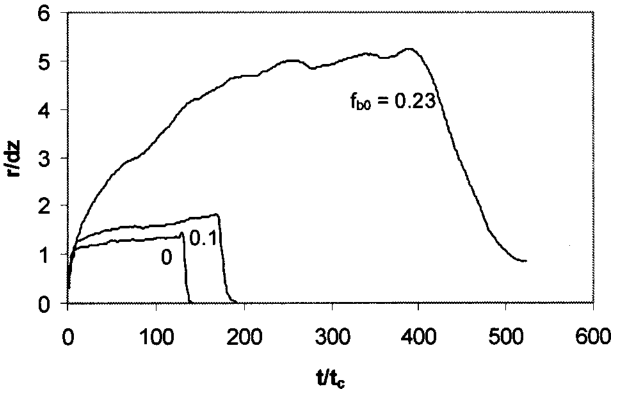

FIG. 12. Effect of the degree of blocking, f_{b0}, on a dimensionless plot of roughness, r, vs time, t ($f_c=0.4$, DP=10, $f_v=0$, $f_i=0.5$). Each curve is the result of averaging seven simulations.

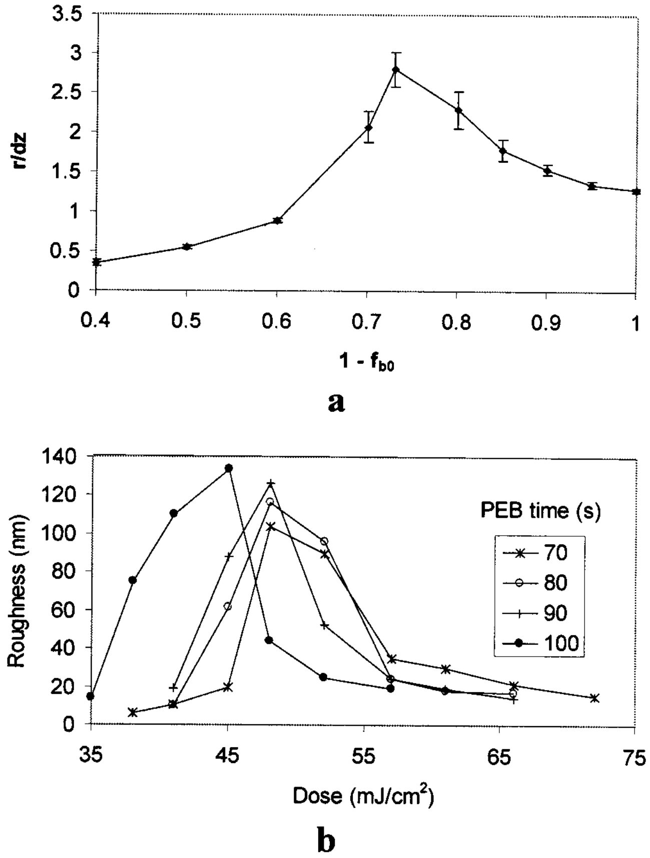

FIG. 13. Comparison of (a) our simulation predictions to (b) experimental results of He and Cerrina (Ref. 1) for the effect of deprotection on surface roughness for a fixed development time. Simulation conditions: $f_c=0.4$, DP=10, $f_v=0$, $f_i=0.5$, $t/t_c=60$.

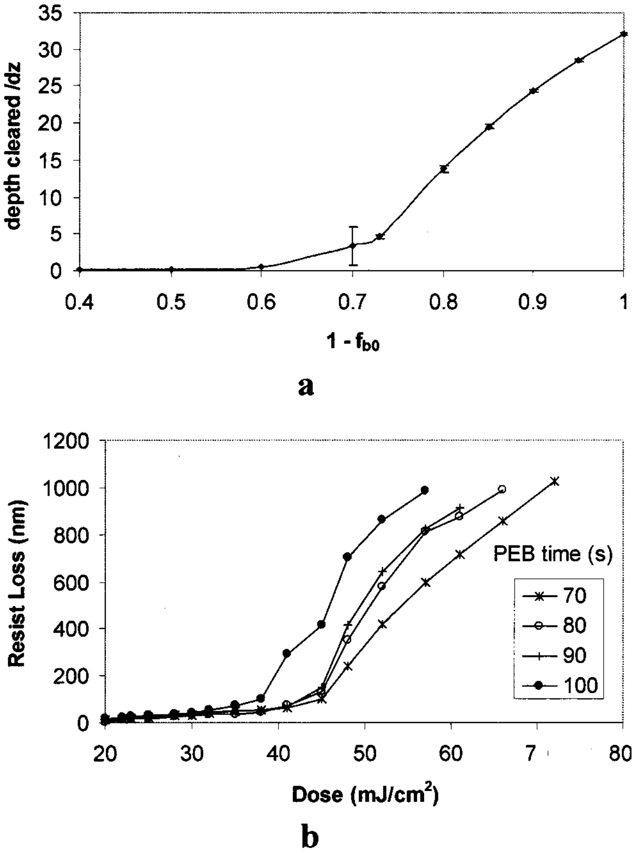

FIG. 14. Comparison of (a) our simulation predictions to (b) experimental results of He and Cerrina (Ref. 1) for the effect of deprotection on depth cleared for a fixed development time. Simulation conditions: $f_c=0.4$, DP =10, $f_v=0$, $f_i=0.5$, $t/t_c=60$.

D. Effect of the void fraction

The simulations described in this article allow a portion of the polymer matrix to be set aside as void space. The specified initial void fraction, f_v, may represent either free volume or residual casting solvent. Void cells automatically convert to developed cells whenever one of their neighboring cells develops.

In Fig. 15 the effect of void space in the polymer matrix on surface roughness is considered. [For reference, the free volume for polymers at the glass transition temperature is 0.025 according to the Williams–Landel–Ferry (WLF) equation.[22]] Increasing the initial void fraction causes the development rate to increase and the surface roughness to decrease. The standard deviation in surface roughness across multiple simulations (not shown) decreases as the initial void fraction increases.

E. Effect of the developer concentration

In Reynolds and Taylor's initial AFM examination of the effect of developer concentration on roughness,[2] the surface roughness of the unexposed portion of a chemically amplified resist was measured following a development time long enough for complete etching of the exposed portion of the photoresist. In later studies,[3,4] the same investigators examined the effect of developer concentration on roughness as a function of development time. Under both the earlier and later sets of conditions, surface roughness was observed to

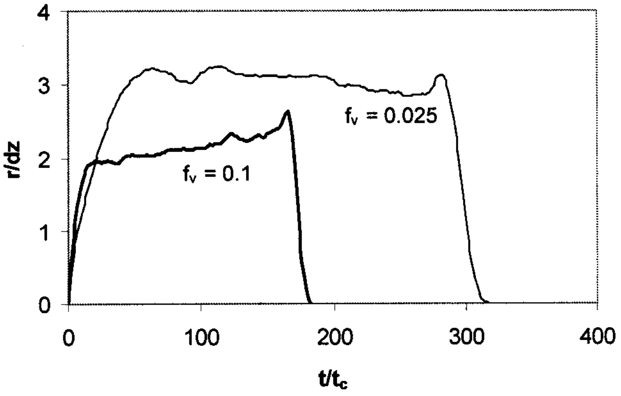

FIG. 15. Effect of void fraction, f_v, on a dimensionless plot of roughness, r, vs time, t ($f_c=0.4$, DP=40, $f_{b0}=0$, $f_i=0.5$). Each curve is the result of averaging seven simulations.

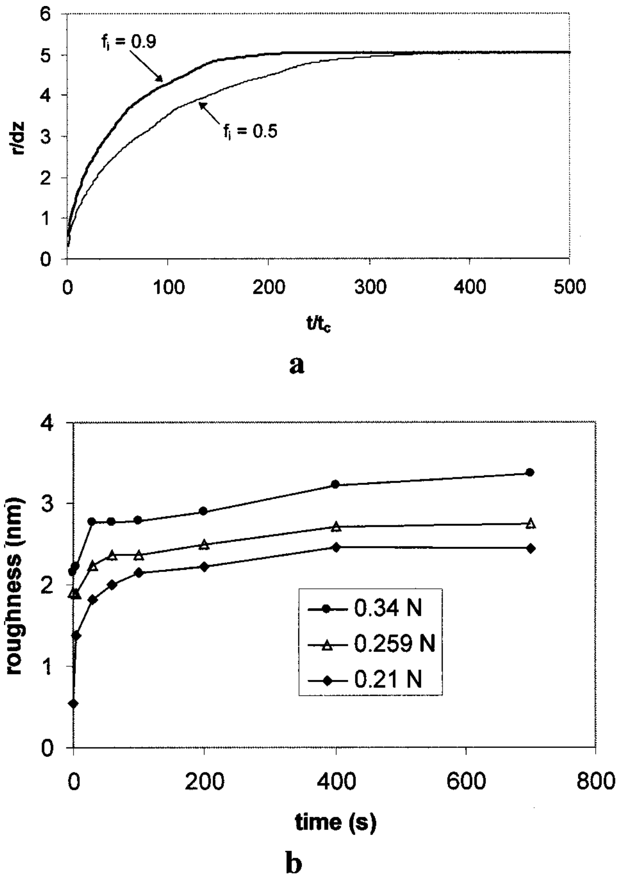

FIG. 16. Comparison of (a) our simulation predictions to (b) experimental results of Reynolds and Taylor (Refs. 2–4) for the effect of developer concentration on roughness as a function of development time. Simulation conditions: $f_c=0.4$, DP=10, $f_{b0}=0.27$, $f_v=0$. Each curve is the result of averaging seven simulations.

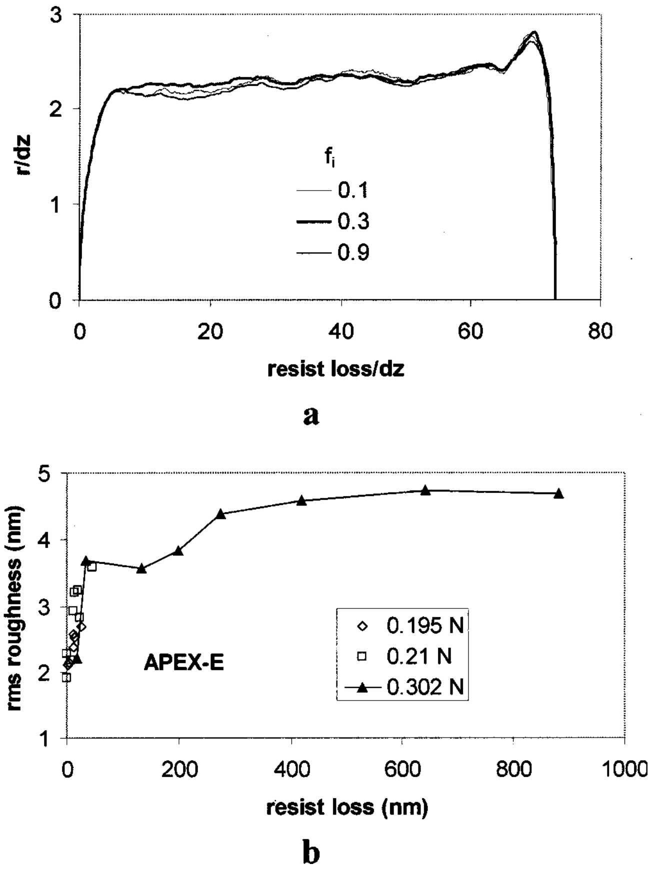

FIG. 17. Comparison of (a) our simulation predictions to (b) experimental results of Reynolds and Taylor (Refs. 2–4) for the effect of developer concentration on roughness as a function of resist loss. Simulation conditions: $f_c=0.4$, DP=30, $f_{b0}=0$, $f_v=0$. Each curve is the result of averaging seven simulations.

increase with developer concentration, whereas the sidewall roughness appears to be independent of developer concentration.

For comparison, our simulation uses a partially blocked matrix to portray the unexposed portion of the photoresist. The simulation parameter analogous to developer concentration is f_i, which is the probability of ionization for a cell in contact with developer. Greater values for f_i correspond to higher developer concentrations. In Fig. 16, the simulated predictions for roughness as a function of development time and f_i are compared to recent AFM measurements[3] of roughness as a function of development time and developer concentration. Increasing f_i causes the roughness in the simulations [Fig. 16(a)] to develop at a faster rate, but roughness eventually reaches an asymptotic value that is independent of f_i. If development is interrupted before a critical time has elapsed, surface roughness in the simulations appears to increase with increasing developer concentration. If the surface roughness measurements are taken after the critical time, surface roughness in the simulations appears to be independent of developer concentration. One would expect the critical time to be less for a lower degree of blocking. Sidewall roughness may demonstrate the same behavior, and, if so, the model would explain that sidewall roughness has been observed to be independent of developer concentration[2] because the development time has exceeded the critical time for the exposed portion of the photoresist.

Recent AFM measurements by Reynolds and Taylor[4] suggest that roughness increases sharply at first and reaches a level roughness, but the final roughness appears greater for higher developer concentrations [Fig. 16(b)]. Whether these experiments show that the developer concentration increases the rate at which roughness develops remains uncertain.[4] Our model predicts that surface roughness, as a function of resist loss, is independent of developer concentration [Fig. 17(a)]. A plot of the surface roughness data of Reynolds and Taylor[4] versus resist loss also produces a single curve that is independent of developer concentration [Fig. 17(b)]. The results of Fig. 17(b) help to explain Fig. 16: the differences in final resist roughness seen in Fig. 16(b) coincide with varying degrees of resist loss. The dependence of surface roughness on developer concentration arises indirectly through the effect of developer concentration on resist loss.

IV. SUMMARY AND CONCLUSIONS

Photoresist development has been simulated as the molecule by molecule removal of polymer chains from a three-dimensional cubic lattice with a critical-ionization fraction as the criterion for removal. Model predictions for the dissolution rate and surface roughness as a function of development time are presented. The model correctly predicts surface rate inhibition, as evidenced by an induction period, and this phenomenon is shown to correspond to a change in surface roughness (a measure of the area of photoresist exposed to developer). Surface roughness is generally inversely related to the dissolution rate. Polymers with a lower degree of polymerization, narrower polydispersity, and greater void fraction are shown to produce less surface roughness. The model predicts that, as the degree of blocking increases, surface roughness passes through a maximum, and experimental studies confirm this prediction. Recent AFM measurements have confirmed model predictions for the effect of development time on surface roughness. The model predicts that surface roughness develops faster with increasing developer concentration and eventually reaches a maximum that is independent of developer concentration. These model predictions are used to explain differences that have been observed in the responses of top-surface and sidewall roughness to changes in developer concentration.

ACKNOWLEDGMENTS

The authors thank Professor Chih-Kang Shih and Rachel Mahaffy of the University of Texas for assistance with the operation of their AFM. They are grateful to Dongxing He, Professor Francesco Cerrina, Geoffrey Reynolds, and Professor James Taylor of the University of Wisconsin for supplying them with the AFM data. They thank Intel Corporation and the Semiconductor Research Corporation (96-LP-409) for financial support.

[1] D. He and F. Cerrina, J. Vac. Sci. Technol. B **16**, 3748 (1998).
[2] G. Reynolds and J. Taylor, Proc. SPIE **3333**, 916 (1998).
[3] G. W. Reynolds and J. W. Taylor, J. Vac. Sci. Technol. B **17**, 334 (1999).
[4] G. W. Reynolds and J. W. Taylor (personal communication).
[5] T. Yoshimura, H. Shiraishi, J. Yamamoto, and S. Okazaki, Jpn. J. Appl. Phys., Part 1 **32**, 6065 (1993).
[6] R. Guerrieri and A. R. Neureuther, IEEE Trans. Comput.-Aided Des. **7**, 755 (1988).
[7] P. Trefonas III, Proc. SPIE **1086**, 484 (1989).
[8] E. W. Scheckler, S. Shukuri, and E. Takeda, Jpn. J. Appl. Phys., Part 1 **32**, 327 (1993).
[9] L. W. Flanagin, V. K. Singh, and C. G. Willson, J. Polym. Sci., Part B: Polym. Phys. **37**, 2103 (1999).
[10] P. C. Tsiartas, L. W. Flanagin, C. L. Henderson, W. D. Hinsberg, I. C. Sanchez, R. T. Bonnecaze, and C. G. Willson, Macromolecules **30**, 4656 (1997).
[11] A. R. Neureuther and C. G. Willson, J. Vac. Sci. Technol. B **6**, 167 (1988).
[12] For filling the lattice with polymer chains, one may use alternative methods that allow control of the chain length distribution and more accurately account for excluded volume effects. The authors are currently studying the application of this technique to the systems described in this article.
[13] K. Kremer and G. S. Grest, in *Monte Carlo and Molecular Dynamics Simulations in Polymer Science*, edited by K. Binder (Oxford University Press, New York, 1995), p. 199.
[14] C. L. McAdams, L. W. Flanagin, C. L. Henderson, A. R. Pawloski, P. Tsiartas, and C. G. Willson, Proc. SPIE **3333**, 1171 (1998).
[15] L. W. Flanagin, C. L. McAdams, W. D. Hinsberg, I. C. Sanchez, and C. G. Willson, Macromolecules (in press).
[16] S. Nonogaki, M. Hashimoto, T. Iwayanagi, and H. Shiraishi, Proc. SPIE **539**, 189 (1985).
[17] R. A. Arcus, Proc. SPIE **631**, 124 (1991).
[18] T. Long and F. Rodriguez, Proc. SPIE **1466**, 188 (1986).
[19] P. C. Tsiartas, L. L. Simpson, A. Qin, C. G. Willson, R. D. Allen, V. J. Krukonis, and P. M. Gallagher-Wetmore, Proc. SPIE **2438**, 261 (1995).
[20] G. G. Barclay, C. J. Hawker, H. Ito, A. Orellana, P. R. L. Malenfant, and R. F. Sinta, Proc. SPIE **2724**, 249 (1996).
[21] G. M. Wallraff, J. Opitz, G. Breyta, H. Ito, and B. Fuller, Proc. SPIE **2724**, 149 (1996).
[22] M. L. Williams, R. F. Landel, and J. D. Ferry, J. Am. Chem. Soc. **77**, 3701 (1955).